

## **Annex 2**

### **EXPERIMENTAL TECHNIQUES**

In this chapter we describe the techniques and relevant parameters of the processes of production and characterization of our materials. Firstly, the technique of ball milling is briefly reviewed, emphasizing those aspects that are more important from the point of view of sample preparation. Afterwards, the main characterization techniques that we have utilized will be studied, starting from the fundamental principles and, when needed, the reader is addressed to the corresponding annexes for further details.

#### **2.1.- Materials processing**

The processing of FM-AFM composites (mainly Co-NiO, SmCo<sub>5</sub>-NiO and SmCo<sub>5</sub>-CoO) was carried out by means of a ball milling process. However, the different structural and magnetic behaviors of Co and SmCo<sub>5</sub> made it necessary to adapt in each case the processing route to optimize the effects of the coupling. In the case of ball milled Co + AFM (NiO or FeS) a heat treatment process (annealing + field cooling to room temperature) of as-milled powders was needed in order to induce FM-AFM exchange interactions, which resulted in improved magnetic properties [1-4]. The as-milled powders were annealed in a vibrating-sample magnetometer (VSM), under vacuum, for 0.5 h at different temperatures,  $T_{ANN}$  ( $300\text{ K} < T_{ANN} < 850\text{ K}$ ) and field cooled using a magnetic field of 5 kOe to room temperature. Occasionally, field cooling procedures in different magnetic fields were also carried out to study the thermal stability or the effect of the cooling field on the exchange coupled composites [4].

However, in the case of SmCo<sub>5</sub> + AFM (NiO or CoO) powders, heating resulted in a rapid deterioration of the hard FM properties. Nevertheless, in SmCo<sub>5</sub> + CoO, some field cooling experiments to 30 K were carried out in an extracting magnetometer setup, applying a field  $H = 50\text{ kOe}$ , in order to observe the effects of the coupling between SmCo<sub>5</sub> and CoO [5,6]. Cooling to low temperatures was required in this case since  $T_N(\text{CoO}) = 290\text{ K}$ .

## **2.1.1.- Mechanical milling**

### **2.1.1.1.- Origins and fundamentals of the technique**

Although a large variety of milling devices had been used in the past for the synthesis and processing of, for example, several types of medicines, foods and many other substances, it was not until the 60's when mechanical alloying was first developed at an industrial scale [7]. Benjamin and co-workers at the *International Nickel Company* used mechanical milling to produce very fine and uniform oxide particles dispersed in nickel-based superalloys. This kind of alloys exhibited high-temperature structural properties that were much better than similar materials produced by conventional metallurgical techniques.

The interest for this technique grew significantly during the 80's, when it was used to synthesize materials in non-equilibrium states [8,9]. Since then, mechanical milling has been successfully utilized to produce many kinds of solid solutions (some of them not obtainable using conventional techniques), disordered and amorphous materials and to induce mechano-chemical reactions, leading to controllable nanostructures, with specific properties [10].

All types of ball milling apparatus, either for industrial production or for laboratory purposes, work in a similar way. Basically, a load powders of one or several materials is introduced in one or more vials, together with some balls and, after appropriate sealing, the vials are agitated or rotated violently, so that the impacts between powders and balls lead to the desired microstructure or reaction for each specific case [10,11].

Among the mechanical milling apparatus that use balls for the grinding (ball mills), the types most commonly used are the following [10] (see figure 2.1):

- *Shaker mills*, for example Spex mills, where the load of powders and balls is stirred by means of a large number of quick vibrations in three orthogonal directions.
- *Attritor mills*, for example the Szegvari attritor, which consists of a stationary vertical cylinder where, the powder and a large number of tiny balls are set into a rotation movement by means of horizontal impulsors, directly attached to the vertical rotation axis (see figure 2.1 (a)).

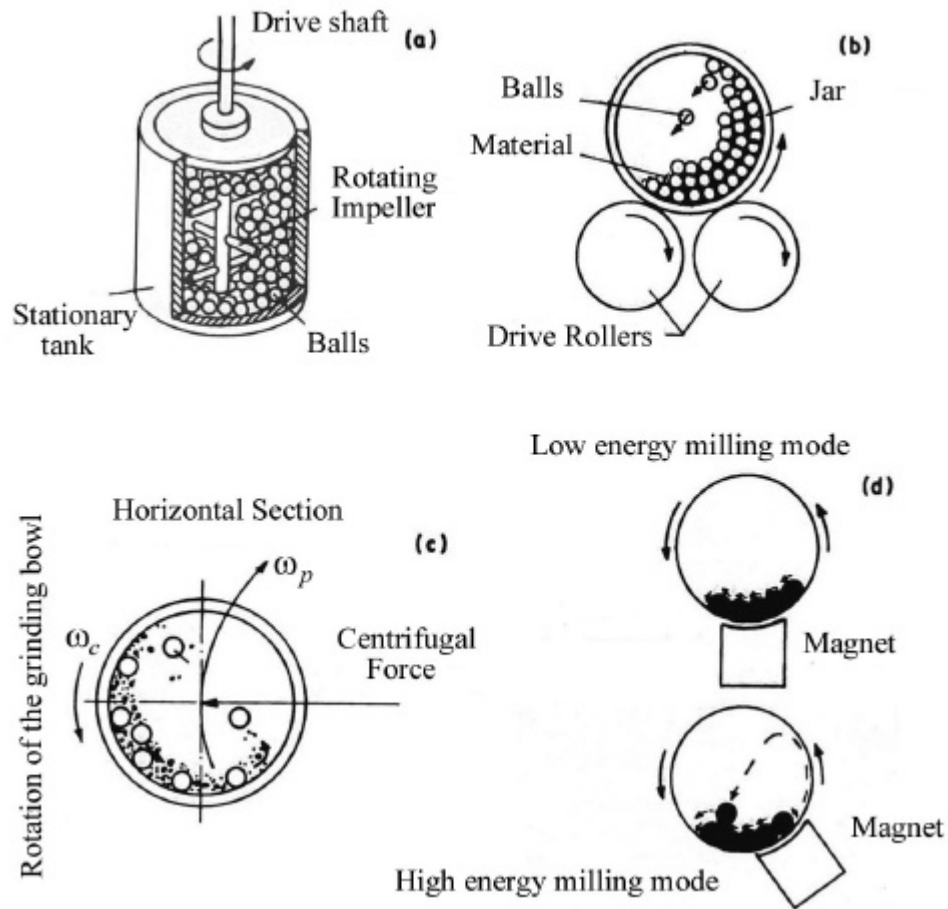


**Figure 2.1:** Schematic diagrams of the balls and powders movements in different types of mechanic mills: (a) attritor mill, (b) rotating trembler mill, (c) planetary mill and (d) magnetic mill [10].

- *Rotating mills*, for example the tumbler mill, where the powder is introduced in a horizontal cylinder containing a number of balls, which by fast rotations create a combination of friction, viscous and gravitational forces that allow the balls to reach speeds up to  $6 \text{ ms}^{-1}$  (see figure 2.1(b)).
- *Planetary mills*, like Fritsch or Retsch mills, where the vials rotate very quickly around their own axis and, simultaneously, around a central axis, similar to a planetary system (see figure 2.1 (c)).

- *Magnetic mills*, for example the uniball Anutech mill, which consist of stainless steel horizontal cylinders with one or more stainless steel balls inside, that rotate fast and, at the same time, move along the vertical plane, due to the presence of a magnetic field, originated from several magnets located at the lower part of the vials (see figure 2.1 (d)).

### 2.1.1.2.- Milling parameters

The experimental parameters that must be taken into account in order to control the final products of a milling process are the following:

- Transferred power
- Milling atmosphere
- Milling media
- Milling temperature

#### Transferred power

Several theoretical models have been developed in order to evaluate the power,  $P$ , transferred to the load during a milling process [12]. According to these models,  $P$  can be estimated using the following expression:

$$P = \mathbf{j} \Delta E N f \quad (2.1)$$

where  $\Delta E$  is the dissipated energy in a system containing  $N$  balls,  $\mathbf{j}$  is a variable less than unity, whose value depends on the volume occupied by the balls inside the vials, and  $f$  is the frequency at which the balls are thrown to the opposite walls of the vials, which in the case of a planetary mill, is a function of the angular speeds of the plate and the vials,  $\omega_p$  and  $\omega_v$ , respectively (see figure 2.1).

If one considers simplified models in which the energy can only be dissipated during the impacts between the balls and the walls of the vials,  $\Delta E$  will only depend on some intrinsic parameters of the planetary mill, such as the distance between the center and walls of the vials and the distance between the center of the disk and the center of the vials. Taking into account the intrinsic characteristics of the planetary mill, there is a number of parameters that can control the final properties of the milled material: the number and mass of the balls, the rotation frequency of the vials, the ball-to-powder weight ratio and the milling time.

### The milling atmosphere

The control of the milling atmosphere is of great importance, since lack of it can lead to some undesired mechano-chemical reactions or contamination in the obtained materials. For example, if the milling is performed in air, one can easily get a significant contamination from oxygen or nitrogen [13]. Sometimes, different types of liquid surfactants are also utilized to avoid powder aggregation during the milling. These liquids can also be an important source of contamination, e.g. C contamination if organic surfactants are used [14]. Usually these effects are not desirable and, therefore, commonly the milling process is carried out under vacuum or in an inert gas, such as argon or helium.

### Milling media

The contamination arising from the milling media (vials and balls) can also be important during the material processing. The amount of this type of contamination depends, among other factors, on how energetic is the mill apparatus and also on the mechanical properties of the powders that are being ground, as well as on the chemical affinity of the material to some of the elements of the milling media. Sometimes, the contamination level can be significantly high. For example, during the synthesis of NiAl alloys from the elemental Ni and Al powders, if stainless steel vials and balls are used, the Fe contamination can reach values of up to 18 % [15]. Sometimes, this problem is minimized using low energetic mills, for example vibratory mills. However, usually, more inert milling media, such as agate, zirconia or tungsten carbide vials and balls are used. Occasionally, the milling media are built up from the same material as the powders, although this can often become technologically difficult and expensive [16].

### Milling temperature:

The exchange of energy during the impacts between powders and balls usually brings about an overall heating of the sample, which can, undoubtedly, affect the microstructure of the as-milled powders [10,16].

This temperature increase can be observed either in the overall milling media, due to the motor or the friction among the several components of the mill (i.e. a macroscopic temperature rise) or locally, at the surface of the particles (i.e. a microscopic temperature rise).

The macroscopic temperature increase that can be observed in the different types of mill apparatus is usually not very high and has been measured by several authors. For

example, the final temperature has been reported to be of up to 50 °C for Spex mills, 172 °C for attritor mills and 120 °C for vibratory mills [10].

Conversely, the microscopic temperature of the powders, just after each impact, can be really high. In fact, it is impossible to directly measure this temperature and, therefore, its values can only be inferred by using some theoretical models or by the microstructural changes taking place in the powders during the milling. For example, Schwarz and Koch estimated a temperature increase (with respect to room temperature) of 350 °C for Spex-type mills [17]. Moreover, Magini *et al.* calculated that the temperature rise could reach up to 400 °C for planetary mills [18].

Although a wide range of microscopic temperature increases have been reported in the literature, it is worth mentioning that, occasionally, the macroscopic temperature (and to certain extent the microscopic one) can be controlled by means of furnaces or refrigerating circuits [10].

### **2.1.1.3.- Temporal evolution of the microstructure**

Usually, in materials subjected to mechanical work in high energetic mill, the final distribution, after long-term milling, of particle sizes and shapes, i.e. the microstructure, becomes rather stable, due to the continuous processes of fracture and soldering. The particle size distribution and particle morphology depend on the kind of material being processed as well as the milling intensity, the ball-to-powder weight ratio, temperature, etc. However, the homogenization process varies depending on the ductility or brittleness of the milled powders. Thus, typically, very different microstructures are obtained when the precursor powders are ductile, brittle or two-component brittle-ductile.

#### **a) Ductile-ductile precursors**

The majority of alloys synthesized by ball milling correspond to this category. As examples of ductile-ductile components that homogenize to different final states we can for example refer to Co-Mn, which forms solid solutions for certain composition ranges [19], Al-25at%Fe which becomes a solid solution [20], or Fe-Zr, which tends to amorphize in the central part of the phase diagram [21].

In this case, the particles first increase in size, up to a maximum value and tend to progressively reduce to some “pseudoequilibrium” dimension. This behavior can be interpreted as the interplay between fracture and soldering mechanisms. Hence, during the

first milling stages, due to the ductility of the powders, soldering predominates over fracturing. However, for longer milling times, both processes tend to reach some equilibrium, leading to a stationary particle size distribution.

Moreover, during the milling, the particles first become elongated and later they develop in platelet or laminar shapes, and even, sometimes, a kind of “sandwich” microstructure can be observed for two or more ductile components. As the milling time increases, the interlaminar distances decrease, the microstructure becomes more and more refined and, finally, homogenization is reached [10,16].

### b) Brittle-brittle precursors

In the first studies of mechanical milling of brittle-brittle components it was thought that for this kind of materials, the milling could only induce fragmentation of the individual particles, without any alloying between them, until the so-called *powderization limit*, where the particle size did not further decrease [10]. However, in the Si-Ge system, it was observed that some alloying was possible since, for certain composition ranges, a solid solution was obtained [22]. Some amorphous alloys have also been formed by milling mixtures of NiZr<sub>2</sub> and Ni<sub>11</sub>Zr<sub>9</sub> [23]. Nevertheless, the mechanisms that govern the formation of alloys in these type of compounds, have not been elucidated, although it seems that a necessary requirement is to have some thermal activation that allows diffusion between the different elements during the milling.

The microstructure of these composites changes with milling time. In general, for short milling times, the particles drastically reduce in size and, at intermediate milling stages, some heterogeneous agglomerates, with granular morphology, of a few  $\mu\text{m}$  in size, are formed. In this case, a homogenous microstructure is only occasionally achieved [10].

### c) Brittle-ductile precursors

In this case, during the milling, the ductile powders acquire elongated shapes (*lamellae*), while the brittle counterparts are simply fractured. At intermediate milling times, the ductile grains become embedded in the brittle matrix, forming agglomerates of several  $\mu\text{m}$  in size. This is the typical microstructure developed when milling ceramic with metallic materials, i.e. the so-called *cermets* [24].

Further increase of the milling time makes the ductile lamellae to become closer and thinner, almost irresoluble, while the brittle particles become more and more tiny, finally dissolving among the ductile particles. The final product becomes sometimes completely

homogenized, depending on the relative solubility of the precursors [25]. Therefore, in order to fully homogenize ductile-brittle systems, not only fragmentation of the brittle particles is required but, also, a good solubility of the brittle elements into the ductile components [10].

#### **2.1.1.4.- Experimental method and working conditions**

The processing of the FM particles and the FM-AFM composites has been carried out by means of a planetary *Fritsch Pulverisette 7* mill (see figure 2.2). The milling chamber contains a disk with two symmetrically located vial supports. The disk rotates around a central axis in a programmable speed and, simultaneously, the vials also rotate around their own axis. The rotations of the disk and the vials are opposite in senses, which avoids agglutination of the powders on the walls of the vials. Moreover, the combination of several forces acting inside the vials, allow the balls to reach high kinetic energy values that can be as high as 12 g.

The working conditions used in the present work have been the following:

- Agate vials ( $\text{SiO}_2$ ). Due to their non-magnetic character, the contamination arising from the vials should, a priori, not affect the magnetic properties of the samples, contrary to stainless steel vials. The volume of the vials was 20 ml.
- Agate balls, again to avoid magnetic contamination. The balls were 10 mm in diameter and had a weight of 2 g per ball. Six balls were put in each vial in all the milling processes.
- Ball-to-powder weight ratio: usually 2:1. Some studies on ball milled Co alone were carried out in larger ratios to analyze the effect of the milling intensity on the allotropic phase transformations occurring in Co during the milling. However, to allow better control of the microstructure of as-milled powders, a lower weight ratio (2:1) was preferred.
- Atmosphere inside the vials: inert gas (Ar). The vials, balls and starting powders were previously degassed under vacuum ( $\approx 10^{-2}$  mbar) during approximately 0.5 h and, subsequently, the vials were purged several times, by introducing and removing Ar gas until, finally, an overpressure of Ar was left in order to avoid air to enter inside the vials during the milling process.

- Milling time: the milling time was chosen to be in the range between 0.1 and 30 h in order to control the optimum microstructure for improved magnetic properties. Longer milling times (e.g. 45 h) were only used in ball milled pure Co to study in more detail the influence of prolonged milling on the Co structural properties.
- Milling intensity: the angular frequency of the rotating disk was chosen to be  $\omega_p = \omega_c = 500$  rpm.



**Figura 2.2:** Photograph of the planetary mill used in the present work, a *Fritsch Pulverisette 7*.

Co system:

High purity Co powders [26] (99.5 %, particle size,  $d < 44 \mu\text{m}$ ) were ball milled alone and together with NiO powders [27] (99 %,  $d < 44 \mu\text{m}$ ) in FM:AFM weight ratios of 1:0, 7:3, 3:2, 1:1 and 2:3 [1-4].

SmCo<sub>5</sub> system:

SmCo<sub>5</sub> powders [28] (99 %,  $d < 500 \mu\text{m}$ ) were ball milled alone and together with CoO (99 %,  $d < 44 \mu\text{m}$ ) in the weight ratio of 1:1 and NiO (99 %,  $d < 44 \mu\text{m}$ ) in different FM:AFM weight ratios: 1:0, 3:1, 3:2 and 1:1 [5,6,29].

## **2.2.- Characterization techniques**

Mechanical milling and posterior heat treatments induce several morphological and structural changes in the material, which have been analyzed by means of scanning electron microscopy (SEM) and X-ray diffraction (XRD), respectively. The structural changes occurring in cobalt subjected to ball milling have also been studied by transmission electron microscopy (TEM). The magnetic characterization has been carried out, in ball milled Co + AFM powders, using a vibrating sample magnetometer (VSM) and, in ball milled SmCo<sub>5</sub> + AFM powders, using an extracting magnetometer.

### **2.2.1.- Scanning Electron Microscopy**

#### **2.2.1.1.- Origins and fundamentals of the technique**

In 1835 Knoll demonstrated, theoretically, that it was possible to built up a scanning electron microscope (SEM) [30]. In 1938, Von Ardenne constructed the first prototype [31]. Scanning electron microscopes became elaborated at an industrial scale in 1965, by the *Cambridge Instruments* company. Since then, they have become an essential tool in many fields of scientific research, such as biology or materials science [32-34].

The main characteristic of electron microscopes, compared to conventional optical microscopes, is that they use electrons instead of light and electromagnetic lenses instead of glass lenses. Under certain assumptions, electrons can be considered as waves, with wavelengths much smaller than visible light. This allows the observation of very small structures that would remain unobservable using optical microscopes, due to diffraction effects.

Basically, it is possible to distinguish between: (i) transmission electron microscopy (TEM), where one can directly observe on a fluorescent screen the image obtained by electrons that go through a thinned sample and (ii) scanning electron microscopy (SEM),

where the electron beam scans over the surface of the sample, inducing electronic transitions and reemission of new electrons that can be used to form the image of the scanned surface.

### **2.2.1.2.- Interaction between the electron beam and the sample**

When an electron beam arrives at the surface of a sample, some electrons can penetrate into it. The depth of this penetration directly depends on the atomic number of the constituents of the specimen. The electrons lose their kinetic energy as they go deeper into the sample. In the zone of penetration, a certain number of interactions between the electrons of the beam and the atoms of the sample take place. And, as a consequence, in this zone, several kinds of signals are emitted (see figure 2.3):

- Auger electrons.
- Secondary electrons.
- Backscattered electrons.
- X-rays.
- Transmitted electrons.

#### Auger Electrons

This type of electrons are emitted when an electron of one of the atoms of the specimen, belonging to an external electronic shell, is transferred to an inner shell due to the interaction with the electrons of the incident beam. These electrons have typically low energy values and, therefore, they can only escape the sample from its surface (from a depth range between 0.5 and 2 nm), thus not giving information about more internal parts of the sample. Nevertheless, the energy of this type of electrons is characteristic of the atom that emits them. Thus, these electrons give compositional information of the specimen.

#### Secondary electrons

These electrons originate from the impacts between high energetic incident electrons and the atoms of the specimen. If the energy of the incident electrons is large enough, the electrons of the atoms in the sample may have enough energy to be expelled out. These are the so-called secondary electrons, which have energies in the range of 0-50 eV. The secondary electrons give information about the density of the sample and the surface topography. However, all the information obtained from secondary electrons is restricted to a penetration depth of 10 nm.

### Backscattered electrons

These electrons are originated when the electrons of the incident beam hit the sample but are not able to penetrate it and are consequently reflected back. Therefore their energy depends very much on the energy of the primary incident beam. The information they give also depends on the atomic number of the elements on the surface and also on its topography. Hence, for example the brightness of the image will depend on the atomic number of the specimen since for higher atomic numbers a larger number of backscattered electrons will be obtained.

### X-rays: Energy Dispersive x-ray analyses (EDX)

When an incident electron hits one atom of the sample inducing the emission of another electron, the corresponding “hole” is immediately occupied by a third electron initially located in a more external electronic shell. As a consequence, some energy in the frequency range of x-rays, is emitted. The wavelengths of the emitted x-rays are characteristic of the atoms that compose the sample. Thus, the resulting spectra is often used to make compositional analyses of the material. This process is usually denoted as *energy dispersive x-ray analysis* (EDX). If some regions of the sample are scanned selecting the part of the x-ray spectra corresponding to one of the elements in the sample, it is possible to obtain the distribution of this element at the surface. This technique is commonly known as *x-ray mapping*. Therefore, regions with higher densities of this element will appear as bright in the image, while lack of this element will result in a dark area.

### Transmitted electrons

When the penetration depth of the electronic incident beam is larger than the sample thickness, some electrons are able to go through it, i.e. they are transmitted. These electrons can be detected so as to obtain a two-dimensional image of the internal structure of the sample. Although a detector for transmitted electrons can be incorporated to a scanning electron microscope, it is rather uncommon and specific transmission electron microscopes are more frequently used for this purpose.

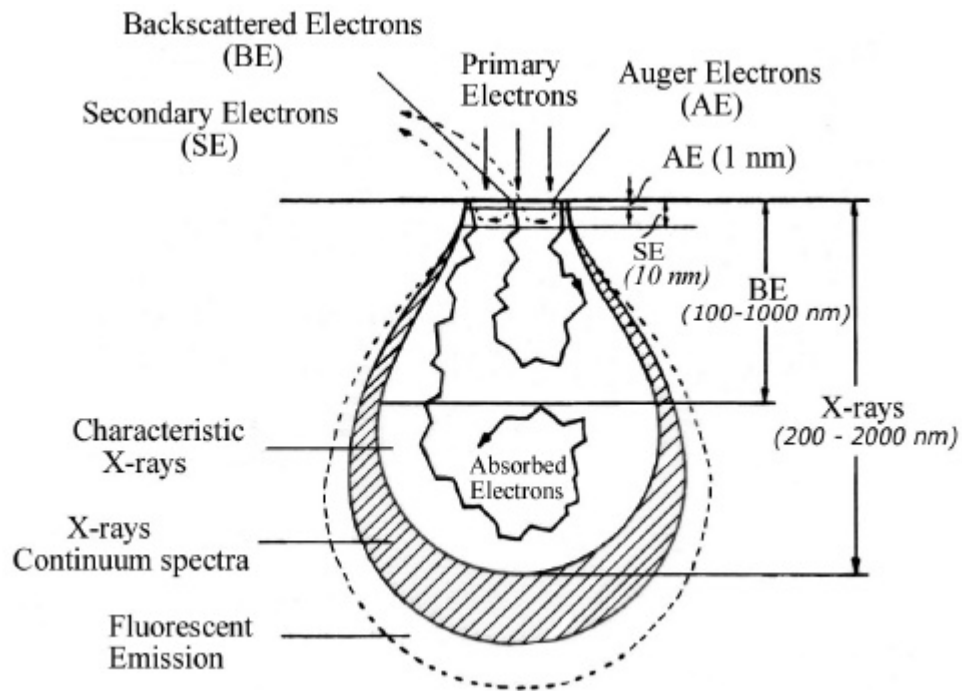


**Figura 2.3:** Types of electrons and radiation generated inside the sample in a scanning electron microscope.

The main components of a scanning electron microscope are:

- Filament.
- System of electromagnetic lenses and diaphragms.
- Sample chamber.
- Scanning generator system.
- Detectors.

When the *filament* (generally a tungsten wire) is heated it produces a beam of electrons, that are accelerated under application of a voltage between cathode and anode, in the range between 1 and 30 kV. Since electrons have a net charge they can be deviated by applying electric and magnetic fields and, therefore, the beam diameter can be significantly reduced by using a system of *electromagnetic lenses*. Moreover, the beam can be further refined and homogenized by means of several metallic *diaphragms*. Furthermore, the

electromagnetic lenses also contribute in accelerating the particles and, thus, they can influence the sharpness of the resultant image.

In the *sample chamber* one can find: the holder, with mechanical mechanisms to move the sample along the three spatial directions and, also, several detectors of the different types of radiation emerging from the sample (x-rays, secondary electrons, backscattered electrons, etc.).

In order to systematically scan the sample, there are two *electromagnetic spirals*, located among the electromagnetic lenses that produce oscillating magnetic fields, along the X-Y directions. This allows precise control of the scan speed.

### **2.2.1.3.- Experimental method and working conditions**

Our observations were carried out using a *JEOL JSM-6300* microscope, located at the *Servei de Microscopia* at the *Universitat Autònoma de Barcelona*. This microscope was equipped with EDX data acquisition system (model *Link Pentafet*).

Although a few images of unmilled and as-milled Co particles were obtained by directly observing the particles spread on the sample holder (and subsequently metallized with Au), in order to observe the interior of the grains and the FM-AFM interfaces, most of the observations were carried out in samples prepared by the following metallographic procedure:

- a) The samples are embedded in a conducting epoxy resin.
- b) They are subsequently polished in order to eliminate the surface of the particles and to be able to observe their interior. This process is first carried out using silicon carbide sand paper. Afterwards a more refined polishing is performed using diamond paste (of 6, 3 and 1  $\mu\text{m}$  in particle size) and 0.3  $\mu\text{m}$  alumina.

The samples were imaged using both secondary and backscattered electrons. Their composition was analyzed by means of Co, Ni and Sm EDX mappings.

### **2.2.2.- Transmission Electron Microscopy**

Although this technique has only been used in this work to study the structural properties of ball milled Co, in this section a brief description of the fundamentals of the technique and the experimental procedure will also be given [35].

In a conventional transmission electron microscope (TEM) a thin specimen is irradiated with an electron beam of uniform current density. The electrons, which are emitted in the electron gun by thermionic emission from tungsten cathodes, have typical energies in the range 60-150 keV. If the penetration depth of the electrons is larger than the thickness of the sample they can go through it. The transmitted electrons are then focused onto a fluorescent screen.

Electrons interact strongly with atoms by elastic and inelastic scattering. The specimens must therefore be very thin, typically of the order of 5 nm – 0.5 μm for 100 keV electrons, depending on the density and elemental composition of the specimen and the resolution desired. Therefore, special preparation procedures are usually required: mechanical thinning, electropolishing, ion milling, etc. However, in the present work, Co particles were so small that they could be directly observed after dispersing them in ethanol in an ultrasonic bath and depositing them onto a TEM grid holder. The TEM utilized in our study was a HITACHI H-7000, located at the *Servei de Microscòpia* at the *Universitat Autònoma de Barcelona*.

Furthermore, TEM observations of as-milled Co powders were complemented by selected area electron diffraction (SAED). To perform this experiment, a selected part of the sample is illuminated with electrons, which, similar to x-ray diffraction (XRD), are diffracted as they go through the sample. The cone of diffracted electrons, which has an amplitude of a few mrad, goes then through a system of electromagnetic lenses and is finally focused onto the screen, giving an image consisting of a combination of spots (for single crystals) and rings (for polycrystals). The diameter of the area selected in our case cannot be decreased below 1 μm owing to the spherical aberration of the objective lens.

If the area illuminated by the electron beam includes a large number of randomly oriented crystallites, then a *powder* pattern is generated. In this case, a family of rings is displayed in the fluorescent screen. The radius  $R$  of a specific ring is related to the  $d$ -spacing of the reflection and the wavelength of the electron beam,  $\lambda$ , by the following relationship:

$$d = \frac{\lambda L}{R} \quad (2.2)$$

where  $L$  is the effective camera length of the electron microscope when used as a diffraction camera. In our case the camera length is of 60 cm. Therefore, by using (2.2) and measuring the relative diameter of the rings it is possible to determine the Miller indexes corresponding to each ring.